NASA Technical Memorandum 85796

Preliminary Indications of Water Film Distribution and Thickness on an Airfoil in a Water Spray

Earl C. Hastings, Jr., and Leonard M. Weinstein

JULY 1984

NASA

NASA Technical Memorandum 85796

Preliminary Indications of Water Film Distribution and Thickness on an Airfoil in a Water Spray

Earl C. Hastings, Jr., and Leonard M. Weinstein
Langley Research Center
Hampton, Virginia

NASA
National Aeronautics
and Space Administration

Scientific and Technical
Information Branch

1984

SUMMARY

Preliminary results are presented from a test to evaluate a sensor for measuring water film thickness. The test was conducted at the Langley Research Center in a small flow apparatus with a model wing in a water spray. The liquid water content was between about 0.5×10^{-3} and 2.6×10^{-3} lbm/ft^3 (8 and 42 g/m^3). The airflow velocities were 81, 112, and 139 ft/sec, and the wing, with a chord length of 1 ft, was at pitch attitudes of 4.0° and 9.3°. Photographic and visual observations were made of the upper wing surface and film thickness was measured on the upper and lower wing surfaces.

The water spray interaction with the wing section resulted in three distinct flow characteristics. Ahead of the wing, a bow wave of water droplets was observed. On the upper wing surface, a continuous water film formed, which had a maximum thickness of about 2 mils at 16.7 percent of the chord length. Finally, between 16.7 and 41.7 percent of the chord length, this continuous film broke down into many discrete runoff streams extending to the wing trailing edge. Measurements on the lower wing surface showed that in general, the continuous film extended further aft than on the upper surface and that the maximum film thickness was about 4 mils at 54.2 percent of the chord length. Increasing the flow velocity or increasing wing pitch attitude significantly decreased the thickness of the continuous film on the forward portion of the wing surfaces.

The performance of the sensor appeared to be highly satisfactory, and where valid comparisons could be made, repeatable results were obtained.

INTRODUCTION

Studies discussed in references 1 and 2 have indicated that heavy rain affects the aerodynamic characteristics of wings and thus may adversely affect aircraft performance. The NASA Langley Research Center and Wallops Flight Center are jointly conducting an experimental investigation of this effect. A paucity of data exists on the characteristics and thickness of water films on wings in heavy rain. This report presents the results of a preliminary study conducted primarily to evaluate a technique for measuring the water thickness on airfoil surfaces. The water thickness data were obtained with a nonintrusive resistance-measuring sensor developed for this test at Langley and described in this report.

SYMBOLS

A	cross-sectional area of spray at the wing location, ft^2
c	wing chord length, in.
LWC	liquid water content, lbm/ft^3 (g/m^3)
Q	flow rate, gal/min or ft^3/sec
q	dynamic pressure, lb/ft^2

R	Reynolds number based on chord length
U	maximum airflow velocity at the centerline, ft/sec
V	voltage output of sensors
x	chordwise location of sensors aft of wing leading edge, in.
α	angle of attack, deg
δ	water film thickness, in.
δ^*	boundary layer displacement thickness, in.
θ	wing pitch attitude relative to tunnel centerline, deg
ρ_w	density of water, lbm/ft^3 (g/m^3)

Subscripts:

max	maximum value measured during a test run
0	zero water film thickness
ref	reference sensor
∞	infinite water film thickness

Abbreviations:

ac	alternating current
dc	direct current
L.E.	leading edge
rpm	revolutions per minute
T.E.	trailing edge

TEST APPARATUS AND CONDITIONS

Test Apparatus

A sketch of the flow apparatus used in these tests is shown in figure 1. The apparatus ingests ambient air from the surrounding room and exhausts it outside the building. The peak airflow velocity was 139 ft/sec. The diameter of the apparatus was 25 in. at the fan and 36 in. at the diffuser exit. The water spray bar and nozzle were located about 8 ft upstream of the exit, and a model wing was located about 1 ft upstream of the exit. Transparent ports near the exit of the flow apparatus allowed photographic coverage and direct viewing of the upper wing surface during testing. A sketch of the water feed system is shown in figure 2.

The wing model was an NACA 0012 airfoil section with a chord length of 12 in. and a span of 33 in. The wing could be set at a pitch attitude of either 4.0° or 9.3° and was fitted with eight sensors to measure water film thickness. The location of these sensors is shown in figure 3.

Sensor

The measuring sensor for water thickness is shown in figure 4. This is a variation of the sensor discussed in reference 3, which was coaxial. The sensor used in the current study consisted of two metal electrodes separated by a nylon insulator. However, the sensor electrodes were aligned relative to the wind, so that the measurements were made at the same chordwise position. The sensor measured the water thickness by measuring the resistance of the water over the electrodes. The circuit used to indicate resistance is shown in figure 5. In order to avoid electrolysis and polarization effects (which cause drift), an ac source (square wave), derived from the first operational amplifier shown in figure 5, was run through the sensor. The signal was amplified and converted to dc by the second operational amplifier in figure 5. The smoothing time constant of 10 msec produced a flat response up to 20 Hz and a usable response up to about 200 Hz.

Output voltage was converted to water thickness by the calibration curve shown in figure 6. This curve was obtained by recording the sensor output with a known thickness of water on the sensor. In this figure, $V - V_0$ is the output voltage of a typical sensor used to measure a thin water film, and $(V_\infty - V_0)_{ref}$ is the output voltage of a reference sensor immersed at a depth which is very large with respect to the distance between the electrodes. This method of calibration accounts for variations in water resistance which may occur during a run or between runs. In this test, the reference sensor was located in a calibration chamber upstream of the spray bar and nozzle (see fig. 2). Although only very thin films were measured in this test, figure 6 shows that the sensor output is linear for $\delta < 0.03$ in. and usable for $\delta < 0.12$ in.

The wing was drilled and slotted to accept the sensor plugs and lead wires, and the electrodes were mounted flush with the surface. After the sensors and leads were inserted, the mounting holes and slots were filled and sanded flush. The wing surface (with the exception of the electrodes) was then sprayed with flat black paint for photographic purposes.

Recorded data consisted of the water flow rate and output voltages from the sensors in the wing and from the reference sensor in the calibration chamber. Water tank pressure and fan rpm were also read from gages and recorded for each run. When the fan speed reached the desired value, the water feed system and data system were turned on. Data were typically recorded for about 20 to 30 sec per run.

Test Conditions

No attempt was made to characterize the spray pattern during these tests. However, unpublished results of earlier tests indicated that the droplet sizes in this apparatus were nearly uniform with diameters of about 15.8 mils, and the spray at the diffuser exit covered an area of about 4.0 ft^2. Test conditions are summarized in table I. To determine data repeatability some test conditions were investigated more than once. Tests were made at wing pitch attitudes of 4.0° and 9.3°. Water tank pressures of 10 and 20 psi resulted in measured water flow rates Q of 3 and 5 gal/min, respectively. Fan speeds of 3000, 4000, and 5000 rpm resulted in maximum velocities (near the tunnel centerline) of $U = 81$, 112, and 139 ft/sec, respectively. Figure 7 shows the variation of dynamic pressure at the diffuser exit. Since the sensors were located in the center of the facility and the primary purpose of these tests was to evaluate the performance of these sensors, the centerline velocity was used to define test conditions.

Values of the liquid water content, LWC, corresponding to the test velocities and water flow rates are shown in figure 8. The values were calculated from

$$LWC = \frac{Q\rho_w}{UA}$$

Since the cross-sectional area of the spray pattern was not measured in these tests, the value of A in these calculations was taken to be 4.0 ft^2 on the basis of the earlier tests. Note that the determination of the absolute value of LWC is subject to considerable error, since the centerline velocity does not act over the entire spray area. However, using an integrated average velocity over the spray area would not influence the relative changes in LWC.

Table II lists the maximum film thickness measured in each test run. When more than one value of δ_{max} was listed in table II for a test condition, the largest value was plotted in this report. Data are not presented for sensor location 6 on the upper surface since this sensor was inoperative when the tests began.

RESULTS AND DISCUSSION

Repeatability

From data obtained from duplicated tests, the performance of the sensor appeared to be highly satisfactory. Although the number of samples is quite low, some indication of the repeatability of the data can be obtained from the δ_{max} data in table II. Comparison of the data from sensor 5 on the upper surface and sensors 1 and 2 on the lower surface shows that the total spread in δ_{max} for each of these individual sensors was never greater than 0.6 mil (±0.3 mil). This is felt to represent a reasonable worse case repeatability for this measurement.

The spread in table II in the δ_{max} data from the other sensors at the same test conditions is sometimes greater than 0.6 mil. This is believed to be the result of the rearward location of these sensors in a region where the film was no longer continuous, but had broken down into runoff streams. As will be discussed later, when this occurred, the sensors could record either no water thickness or the thickness of a random runoff stream.

Photographic and Visual Observations

Visual and photographic observations were made of the upper wing surface. Three distinct types of water flow were observed. The first was a sheath of water in front of the wing, having the appearance of bow wave near the leading edge. This sheath appeared similar to those observed in some earlier tests on radomes in a water spray.

On the wing surface itself, there was a continuous water film near the leading edge, which broke down into a number of runoff streams aft of the continuous sheet.

Figure 9 is a photograph of the wing for $\theta = 4.0°$, $U = 139$ ft/sec, and $Q = 5$ gal/min, and figure 10 is a photograph at the same values of U and Q with $\theta = 9.3°$. Although the sheath of concentrated droplets is not obvious in these figures, the continuous film near the leading edge and the runoff streams are evident at both pitch attitudes. The runoff streams remained attached to the surface all the way to the trailing edge. Figures 9 and 10 are typical of the upper surface patterns, which showed that the continuous sheet did not extend as far aft as $x/c = 41.7$ percent (sensor 7) on the upper surface, but that runoff streams were present at the $x/c = 41.7$ and 54.2 percent. These patterns were established very quickly after the water spray began (within 1 or 2 sec) and remained essentially the same throughout the run. When the continuous film broke down, interpretation of the data was more difficult, since the sensor might record no film thickness or the thickness of a runoff stream. This effect should be kept in mind when evaluating the results presented in the following section.

Photographic and visual observations did not show any significant film cratering due to droplet impacts. This observation is consistent with the result noted in the test of reference 1.

Film Thickness Measurements

Film thickness distribution.- Film thickness measurements are shown for $\theta = 4.0°$ in figure 11 and for $\theta = 9.3°$ in figure 12. (Figs. 11(a) and 12(a) are for $Q = 3$ gal/min and figs. 11(b) and 12(b) are for $Q = 5$ gal/min.)

The available upper surface data in general indicate that the greatest depth of the continuous film was about 2 mils at $x/c = 16.7$ percent and that δ_{max} decreased with increasing distance aft of $x/c = 16.7$ percent. Exceptions to this trend are shown in figure 11(a) at $x/c = 54.2$ percent and $U = 81$ ft/sec, and in figure 11(b) at $x/c = 41.7$ percent and $U = 112$ ft/sec. Since both of these measuring stations were aft of the observed continuous sheet (see figs. 9 and 10), these data are believed to indicate the depth of runoff streams rather than the depth of the continuous film.

The measurements on the lower surface in general show a different trend from those on the upper surface. The preponderance of the measurements indicate that δ_{max} on this surface increased with increasing x/c to locations further aft than on the upper surface. The largest film depths indicated on the lower surface were about 4 mils at $x/c = 54.2$ percent.

It is interesting to observe that at these low Reynolds numbers, the extent and the location of the maximum thickness of the continuous water film are similar to those of the laminar boundary layer. Figure 13 shows the values of δ^* predicted for an NACA 0012 airfoil at $\alpha = 4.0°$ and 9.3°. The predictions were made using the method of reference 4; and the value of R (for $c = 1.0$ ft and $U = 112$ ft/sec) was 7.15×10^5. The calculations show that at both values of α, the laminar boundary layer extends further aft on the lower surface and has a maximum thickness at the point of transition. The similarity between these trends and those previously noted for the continuous water film indicates that boundary layer characteristics may significantly affect the extent and thickness of the water film.

Effect of velocity.- The effect of flow velocity on the film thickness distributions is also shown in figures 11 and 12. In general, all the upper and lower surface measurements show that an increase in velocity resulted in a significant decrease in δ_{max}. Unpublished Langley calculations of water film thickness on spheres in heavy rain have shown that δ decreases when the liquid water content decreases. Increasing flow velocity while maintaining constant Q reduces LWC (see fig. 8) as a result of distributing a given mass of water over larger volumes of air. The data trends in figures 11 and 12, showing decreasing δ_{max} with increasing velocity, are consistent with these calculations.

Effect of pitch attitude.- In figure 14, the film thickness distributions at $\theta = 4.0°$ and $9.3°$ are compared at $Q = 3$ gal/min and $U = 112$ ft/sec. At $x/c = 16.7$, 29.2, and 41.7 percent, increasing pitch attitude significantly decreased film thickness. (No valid comparison can be made at $x/c = 54.2$ percent because at $\theta = 4.0°$, the continuous film had begun to break down prior to reaching this station.)

CONCLUDING REMARKS

Preliminary results have been presented from the test of a sensor for measuring water film thickness in a water spray. The test was conducted in a flow apparatus with a model wing with a chord length of 1 ft at pitch attitudes of 4.0° and 9.3°. Airflow velocities investigated were 81, 112, and 139 ft/sec and water flow rates were 3 gal/min and 5 gal/min. The liquid water content was between approximately 0.5×10^{-3} and 2.6×10^{-3} lbm/ft^3 (8 and 42 g/m^3).

Visual and photographic observations of the upper surface indicated that a water sheath with the appearance of a bow wave occurred ahead of the airfoil leading edge. The forward portion of the surface was covered with a continuous water film, which broke down into many discrete runoff streams extending streamwise to the airfoil trailing edge.

The performance of the sensor appeared to be highly satisfactory, and where valid comparisons could be made, repeatable results were obtained. Water film thickness measurements indicated that the maximum thickness of the continuous film on the upper surface was about 2 mils at the 16.7 percent chord location. The thickness of the continuous film decreased with increasing chord length aft of this location and broke down into discrete runoff streams prior to reaching the 41.7 percent chord location. The measurements on the lower surface in general show a different trend. These data indicate that the thickness of the continuous film increased with increasing chord length to locations further aft than on the upper surface. The largest film depths on this surface were about 4 mils measured at the 54.2 percent chord location. The similarity in the trends of the continuous film distributions and the predicted boundary layer characteristics indicate that boundary layer characteristics may significantly affect the water film characteristics.

Increasing the flow velocity was found to significantly decrease the depth of the continuous water film. Increasing wing pitch attitude also significantly decreased the depth of the continuous water film.

Langley Research Center
National Aeronautics and Space Administration
Hampton, VA 23665
May 29, 1984

REFERENCES

1. Luers, James K.; and Haines, Patrick A.: Experimental Measurements of Rain Effects on Aircraft Aerodynamics. AIAA-83-0275, Jan. 1983.

2. Haines, P.; and Luers, J.: Aerodynamic Penalties of Heavy Rain on Landing Airplanes. J. Aircr., vol. 20, no. 2, Feb. 1983, pp. 111-119.

3. Hammitt, F. G.; Hwang, J. B.; and Kim, W.: Liquid Film Thickness Measurements in University of Michigan Wet Steam Tunnel. Rep. No. UMICH 012449-23-I, Mech. Eng. Dep., Univ. of Michigan, Dec. 1975. (Available from NTIS as PB 247 804.)

4. Stevens, W. A.; Goradia, S. H.; and Braden, J. A.: Mathematical Model for Two-Dimensional Multi-Component Airfoils in Viscous Flow. NASA CR-1843, 1971.

TABLE I.- TEST CONDITIONS

Run	θ, deg	Tank pressure, psi	Q, gal/min	Fan speed, rpm	U, ft/sec
8	4.0	10	3	4000	112
9				5000	139
10				4000	112
11				3000	81
12		20	5	3000	81
13				4000	112
14				5000	139
15				4000	112
16				3000	81
17		10	3	3000	81
18				4000	112
19				5000	139
20				4000	112
21				3000	81
30	9.3	10	3	3000	81
31				4000	112
32				5000	139
33				4000	112
34				3000	81
35		20	5	3000	81
36				4000	112
37				5000	139
38				4000	112
39				3000	81

TABLE II.- MEASURED MAXIMUM FILM THICKNESS

θ, deg	Q, gal/min	U, ft/sec	Run	δ_{max}, mils						
				Lower surface sensors				Upper surface sensors		
				1	2	3	4	5	7	8
4.0	3	81	11	2.1	2.9	3.8	0	1.7	0.8	0
		81	17	2.1	3.0	3.4	.2	2.2	0	0
		81	21	1.8	2.4	3.2	0	2.0	0	1.6
		112	8	1.3	1.7	0	0	1.5	0	0
		112	10	1.5	1.9	.4	.6	1.6	.8	0
		112	20	1.3	1.8	2.1	0	1.3	0	0
		136	9	1.0	1.1	0	0	1.2	0	0
		136	19	1.2	1.2	1.4	0	1.3	0	0
4.0	5	81	12	1.7	2.6	0	0	2.1	0	0
		81	16	1.7	2.2	0	0	1.8	0	0
		112	13	1.6	2.1	2.9	3.4	1.7	0	0
		112	15	1.5	2.2	2.3	3.2	1.3	3.0	0
		136	14	1.2	1.5	1.6	1.6	.6	0	0
9.3	3	81	30	.6	1.4	2.0	3.5	2.0	0	0
		81	34	.8	1.7	2.0	2.5	1.6	0	0
		112	31	0	.9	.9	1.7	0	0	0
		136	32	0	.6	1.2	.9	0	0	0
9.3	5	81	35	.6	1.5	2.2	2.1	.6	0	0
		81	39	1.1	1.8	1.6	2.4	.5	0	0
		112	36	.5	1.2	1.1	2.7	0	0	0
		112	38	.6	1.2	1.7	2.6	.3	0	0
		136	37	.5	.9	.9	1.2	0	0	0

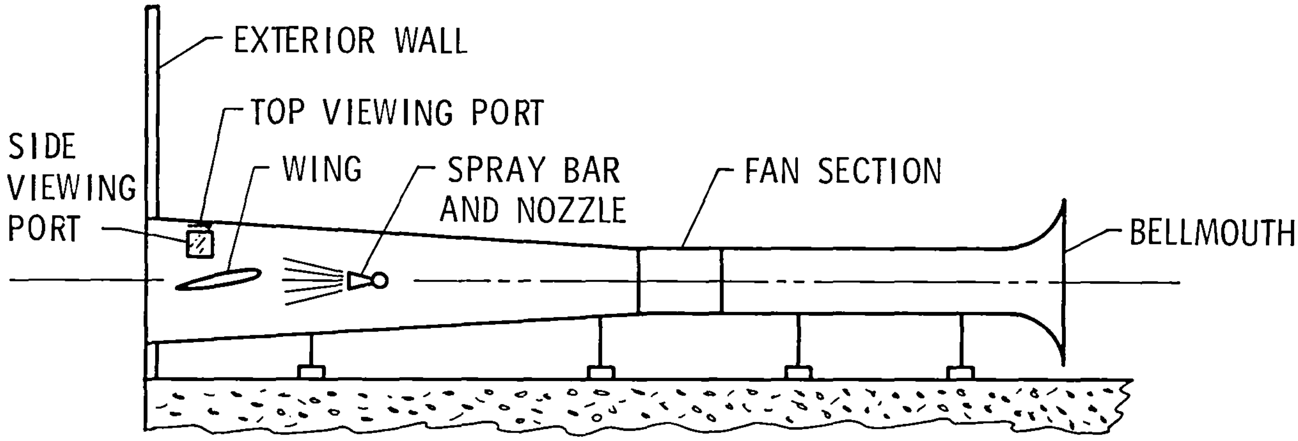

Figure 1.- Sketch of flow apparatus.

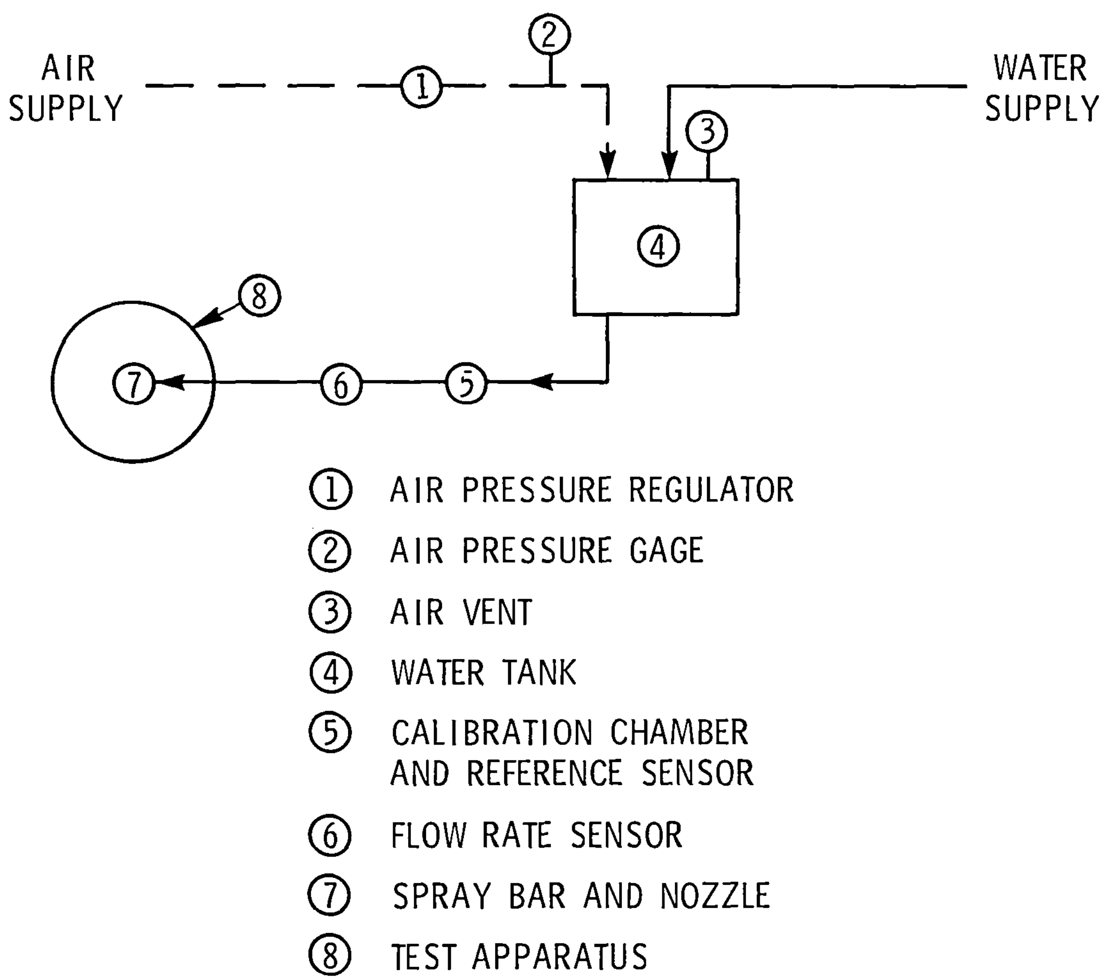

Figure 2.- Diagram of the water feed system.

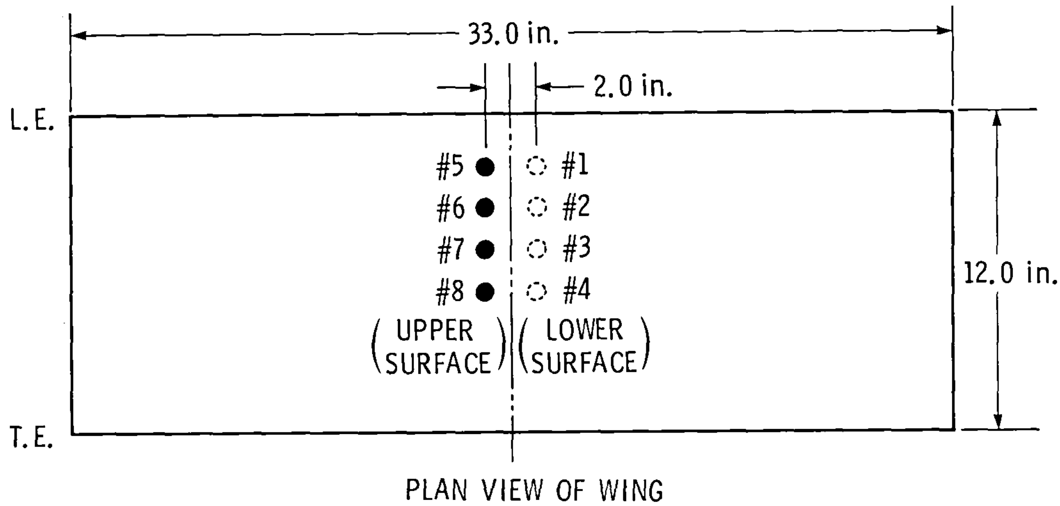

SENSOR NO.	DISTANCE AFT OF L.E., in.	x/c, %
1,5	2.0	16.7
2,6	3.5	29.2
3,7	5.0	41.7
4,8	6.5	54.2

Figure 3.- Location of sensors on wing.

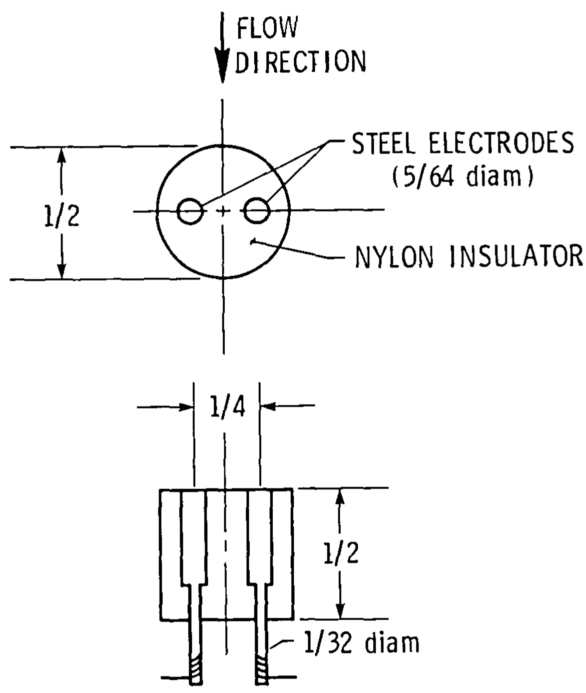

Figure 4.- Sketch of a typical sensor for measuring water thickness. Dimensions are in inches.

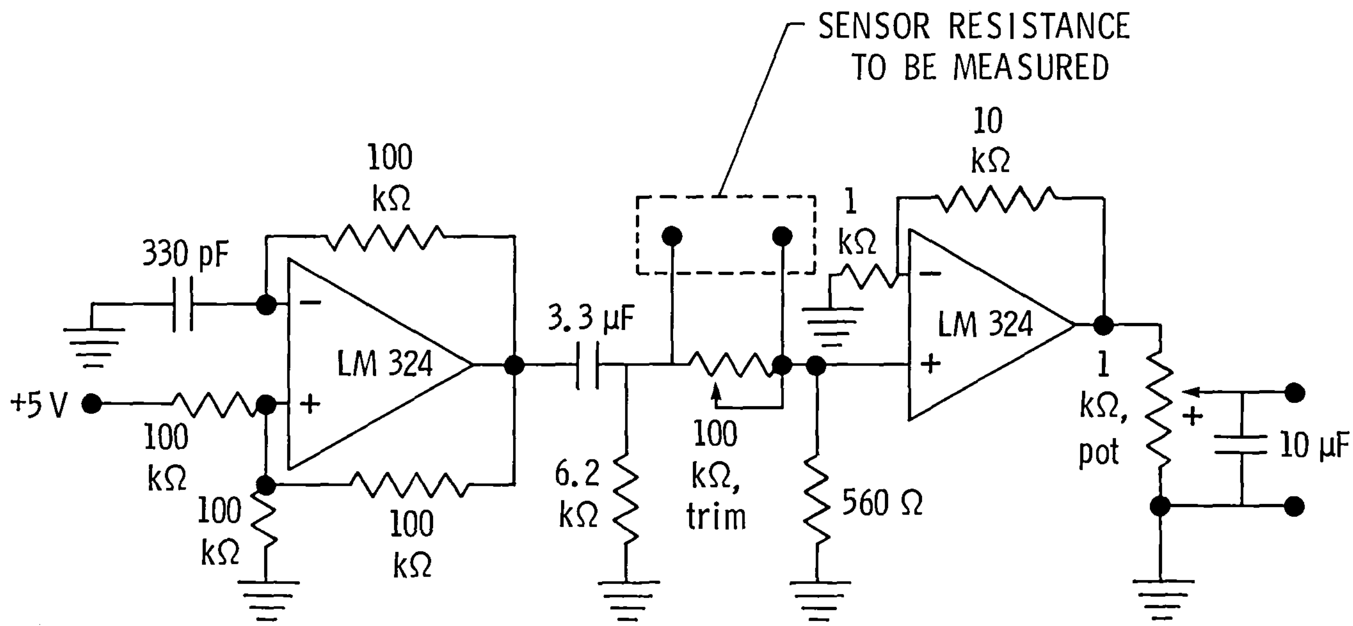

Figure 5.- Resistance-measuring circuit.

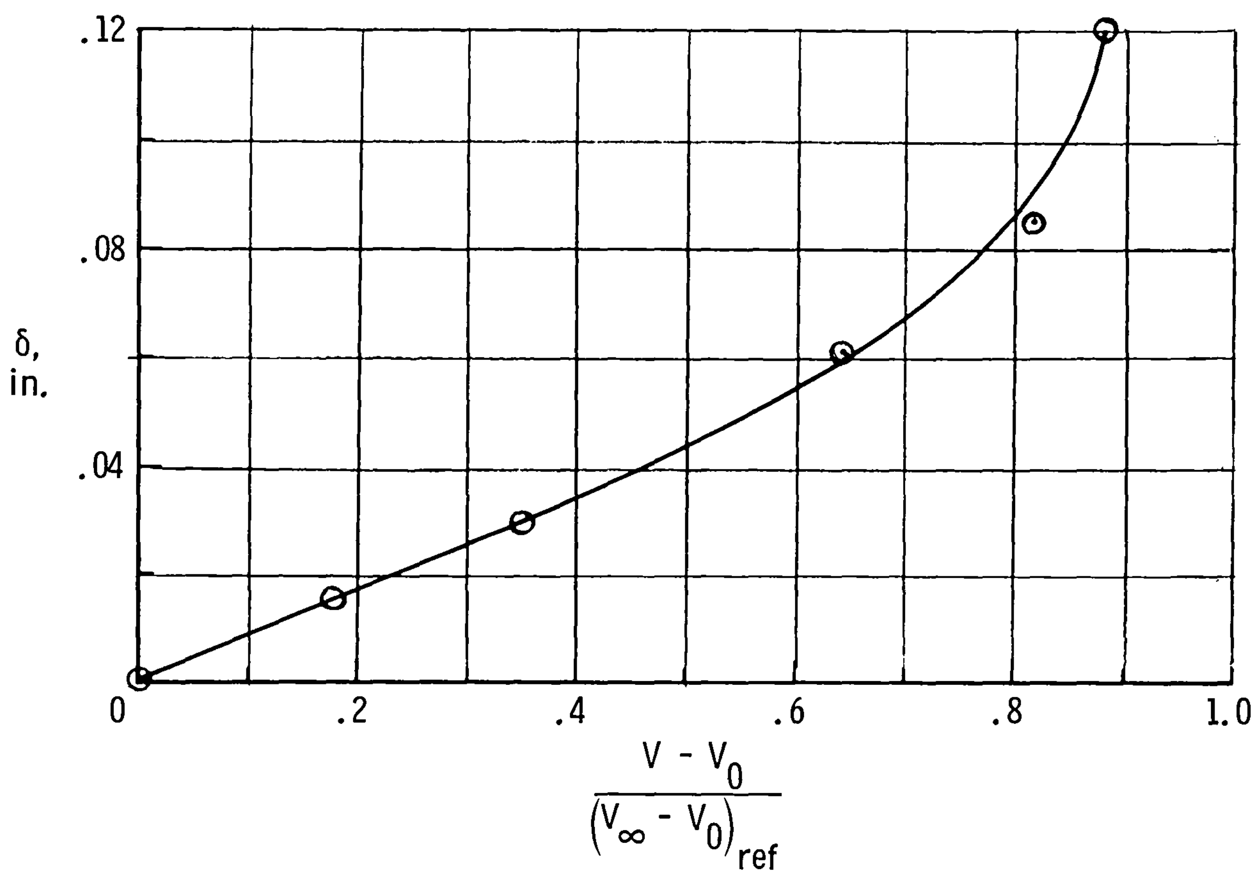

Figure 6.- Sensor calibration curve.

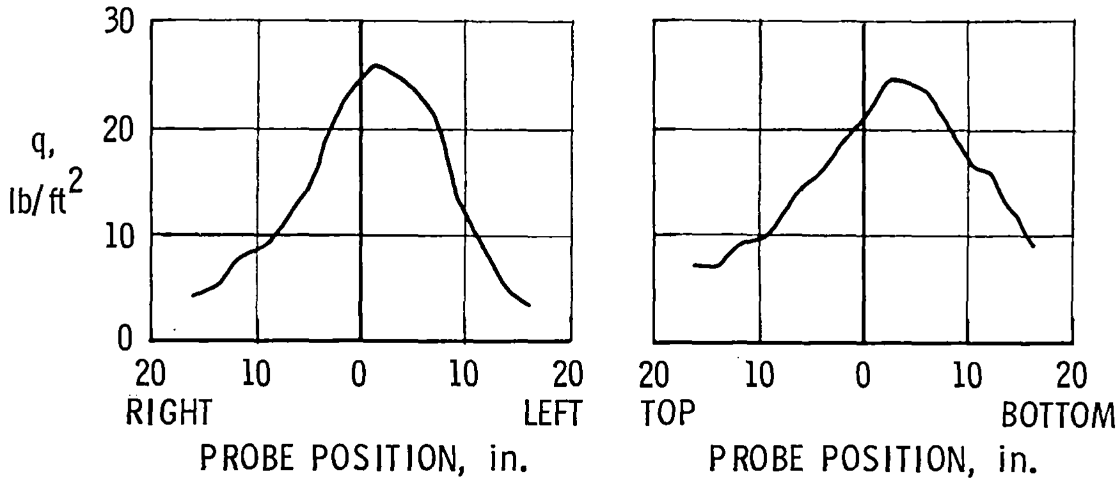

(a) Horizontal probe.

(b) Vertical probe.

Figure 7.- Dynamic pressure measurements at diffuser exit. Fan speed is 5000 rpm.

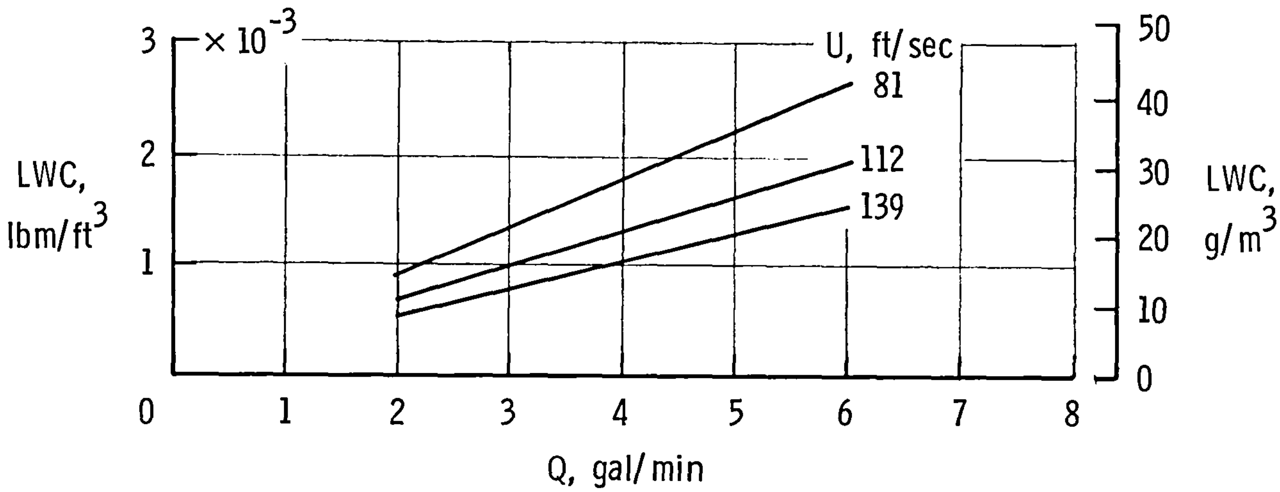

Figure 8.- Variation of liquid water content with test velocity and flow rate of water.

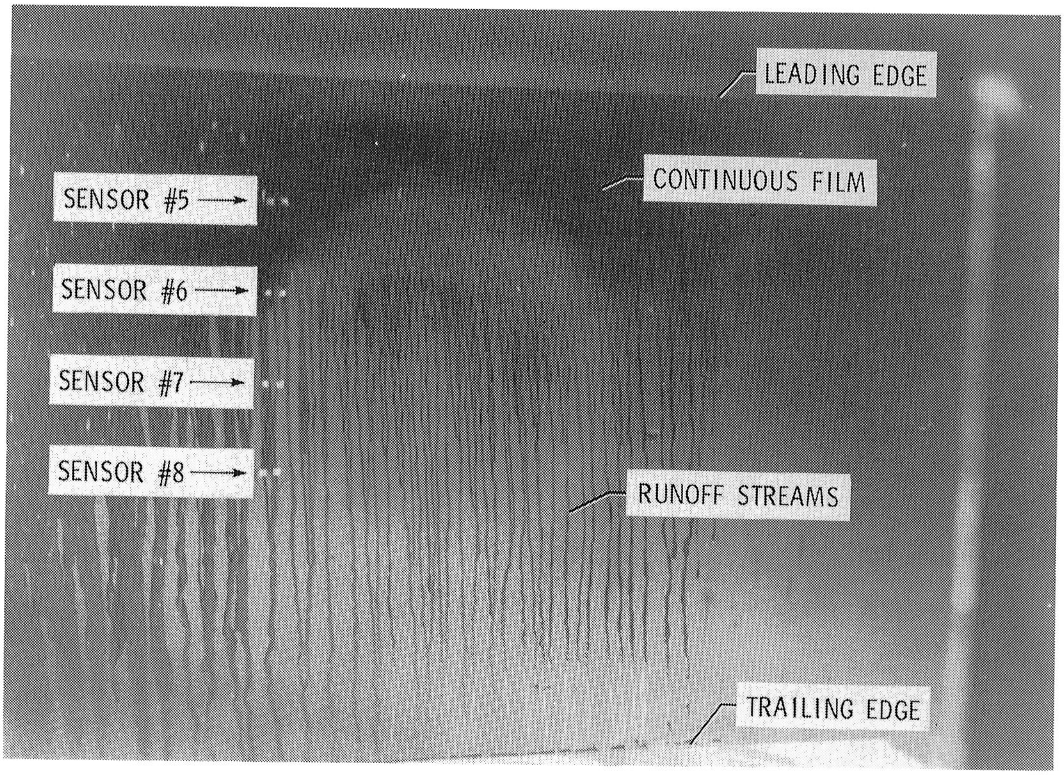

L-84-48

Figure 9.- Typical water film pattern on wing upper surface at $\theta = 4.0°$. U = 139 ft/sec; Q = 5 gal/min.

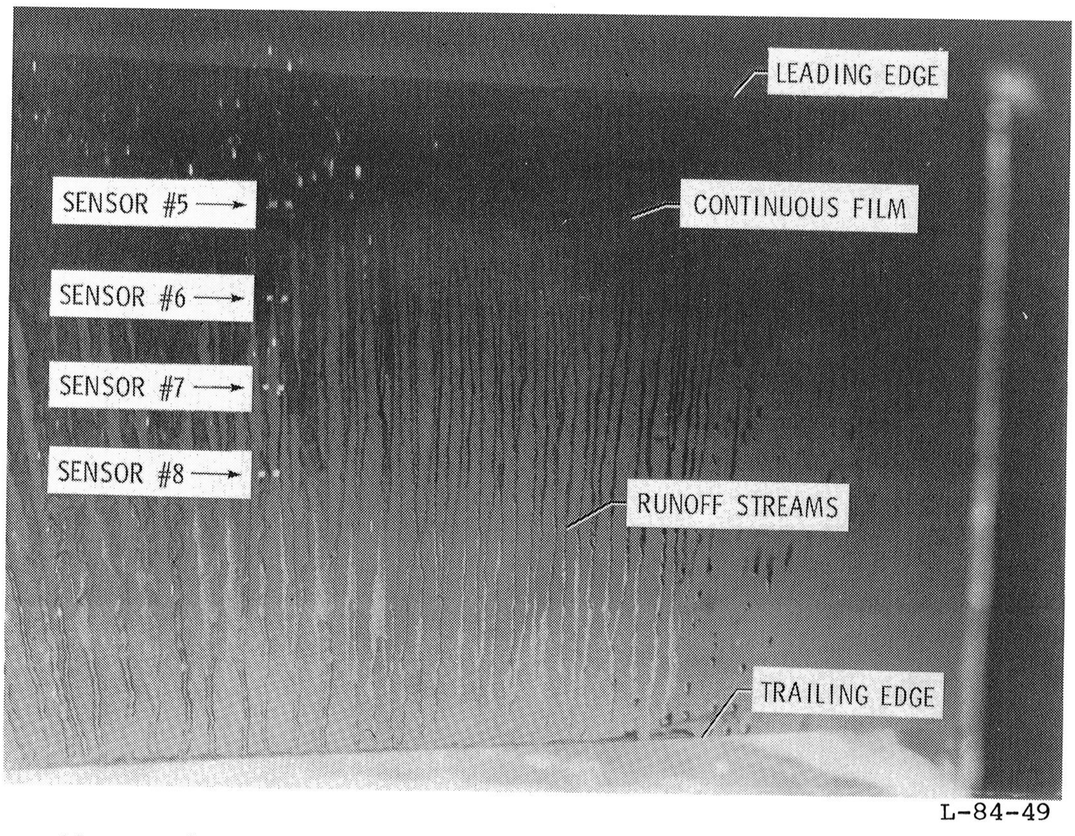

L-84-49

Figure 10.- Typical water film pattern on wing upper surface at $\theta = 9.3°$. U = 139 ft/sec; Q = 5 gal/min.

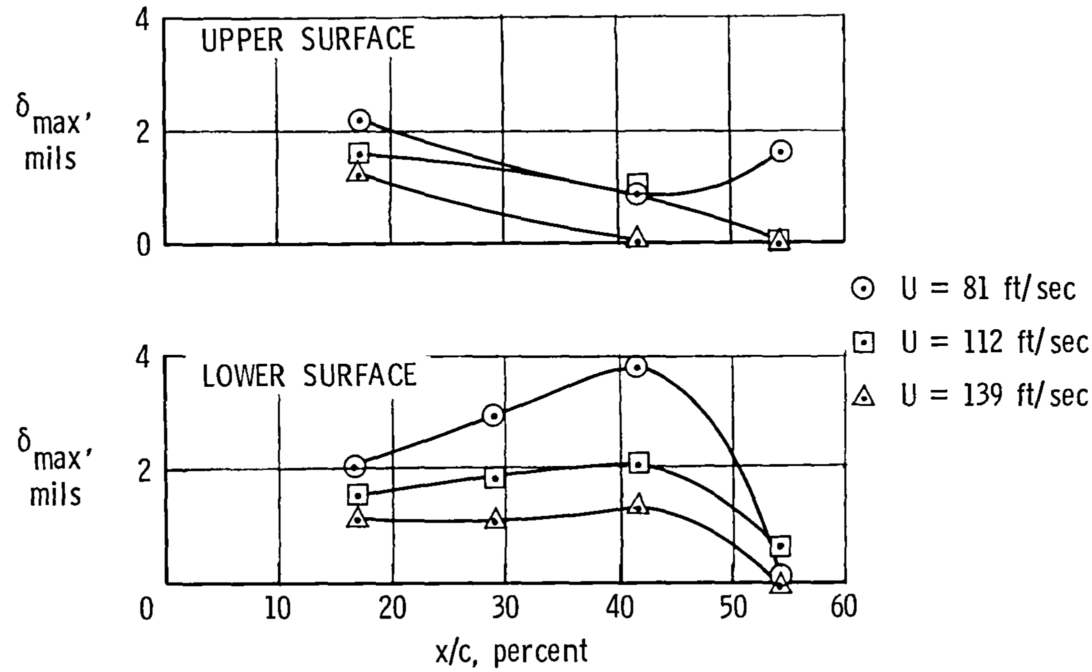

(a) Q = 3 gal/min.

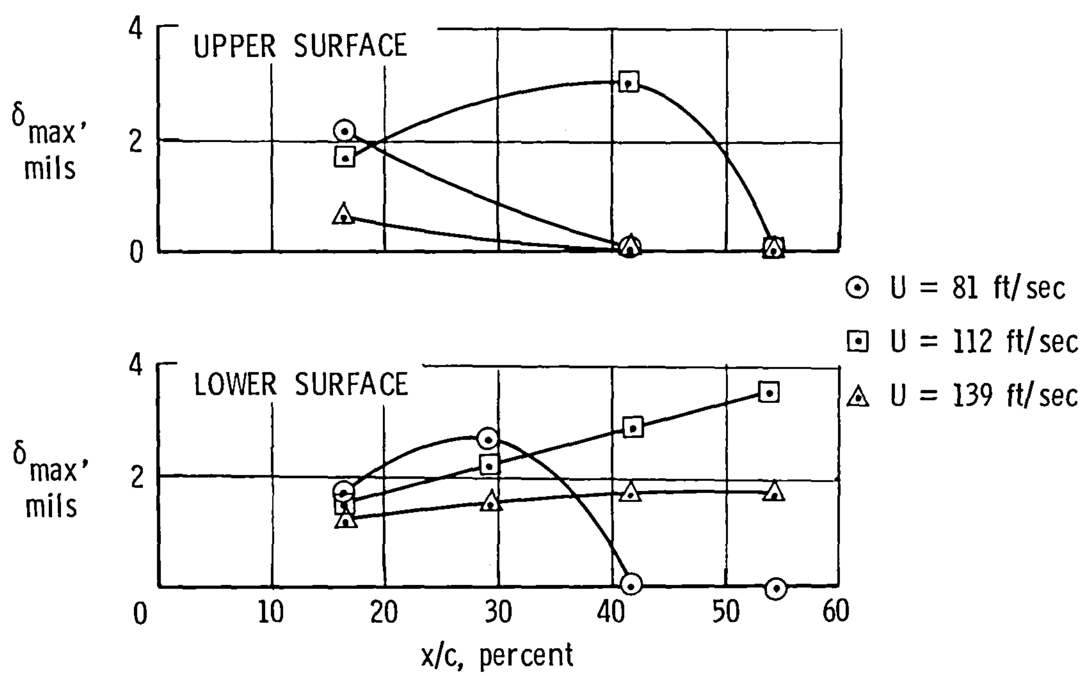

(b) Q = 5 gal/min.

Figure 11.- Film thickness distribution at $\theta = 4.0°$.

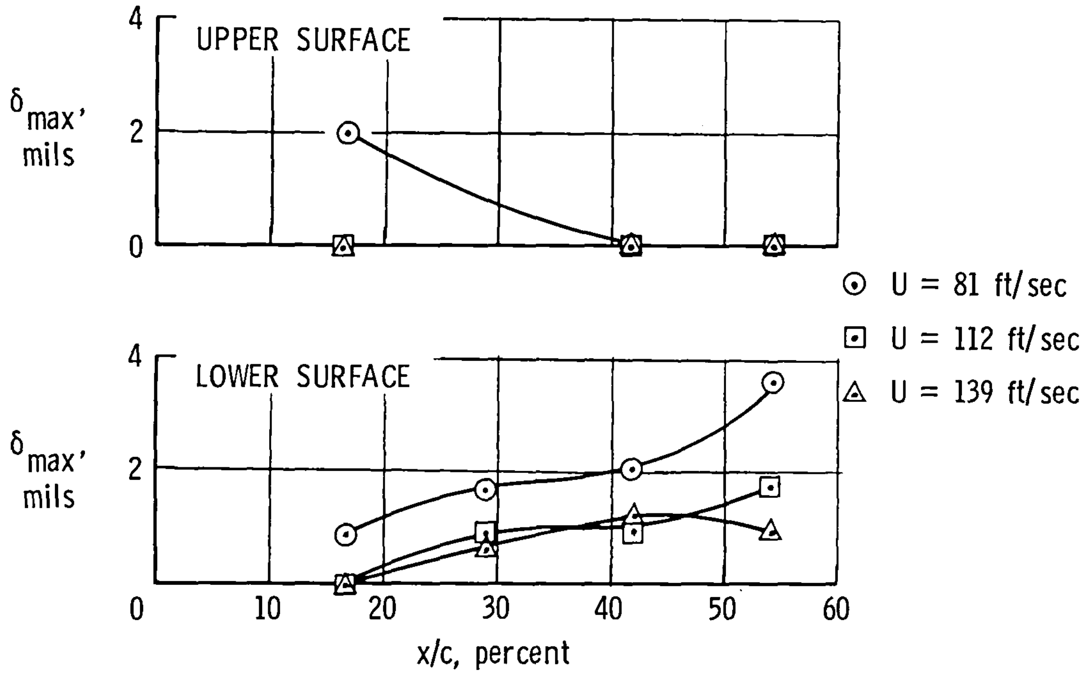

(a) Q = 3 gal/min.

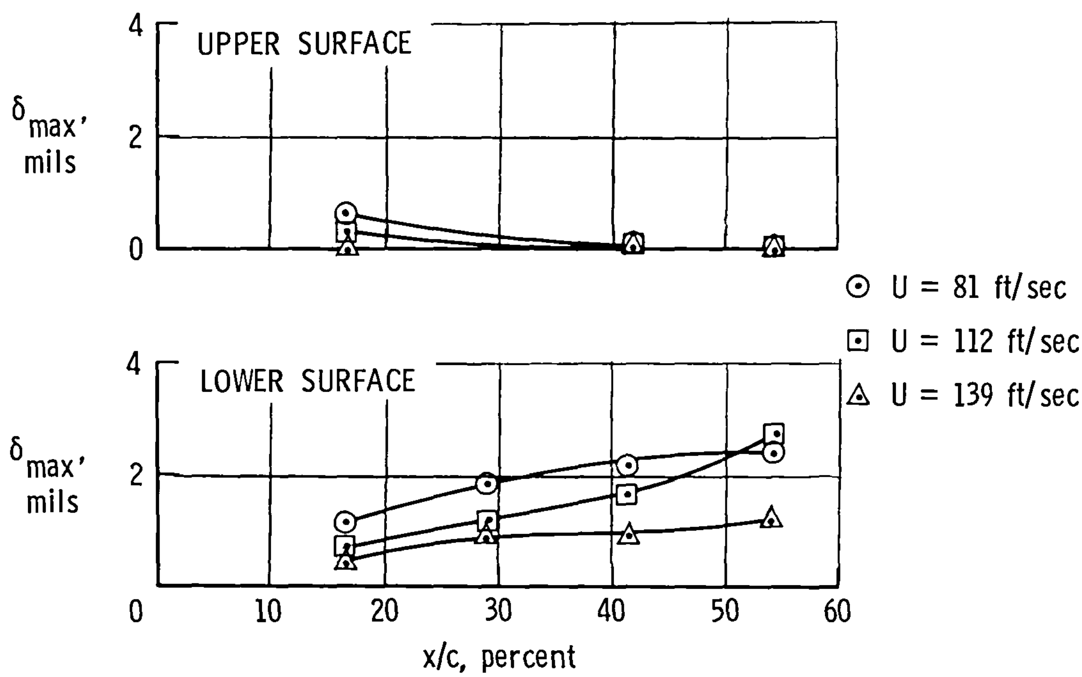

(b) Q = 5 gal/min.

Figure 12.- Film thickness distribution at $\theta = 9.3°$.

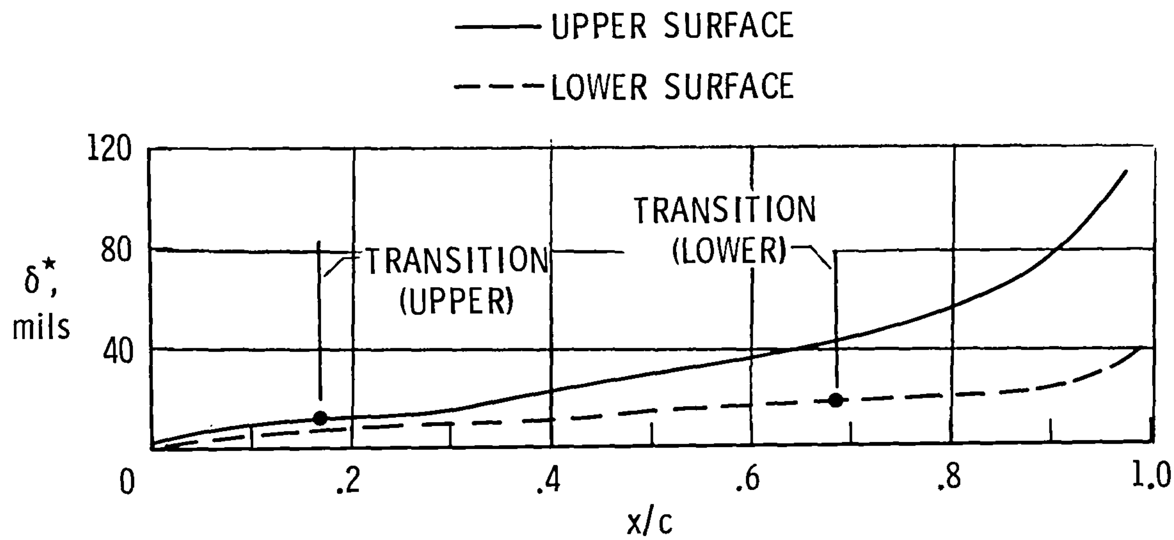

(a) $\alpha = 4.0°$.

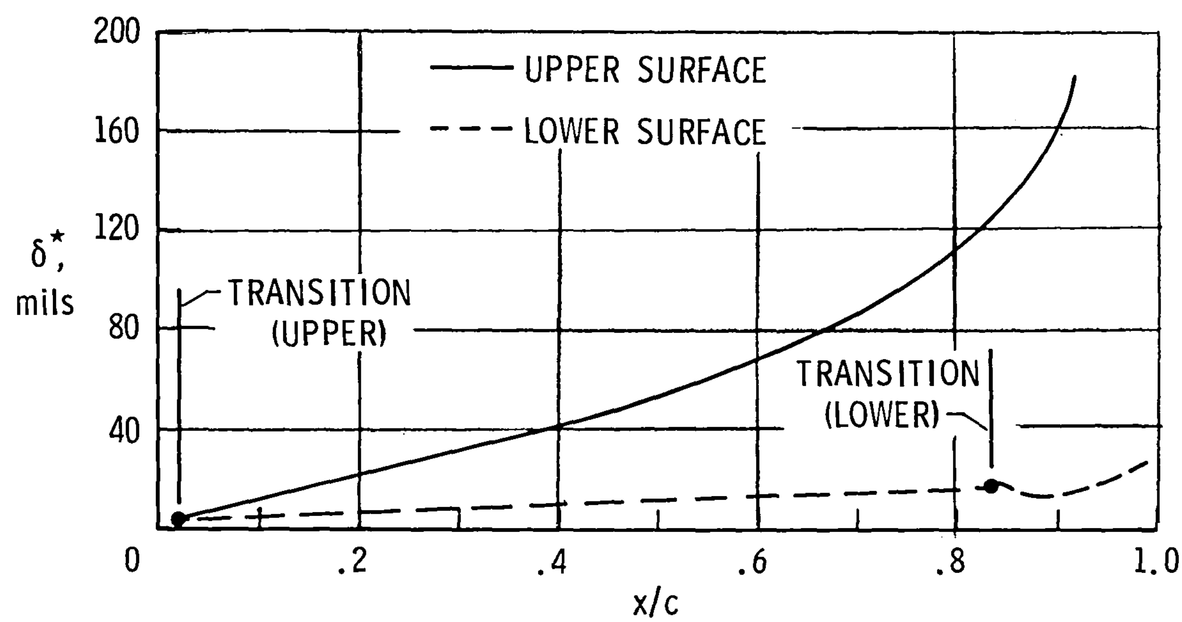

(b) $\alpha = 9.3°$.

Figure 13.- Calculated boundary-layer displacement thickness for two-dimensional NACA 0012 airfoil. $R = 7.15 \times 10^5$; $c = 1.0$ ft; $U = 112$ ft/sec.

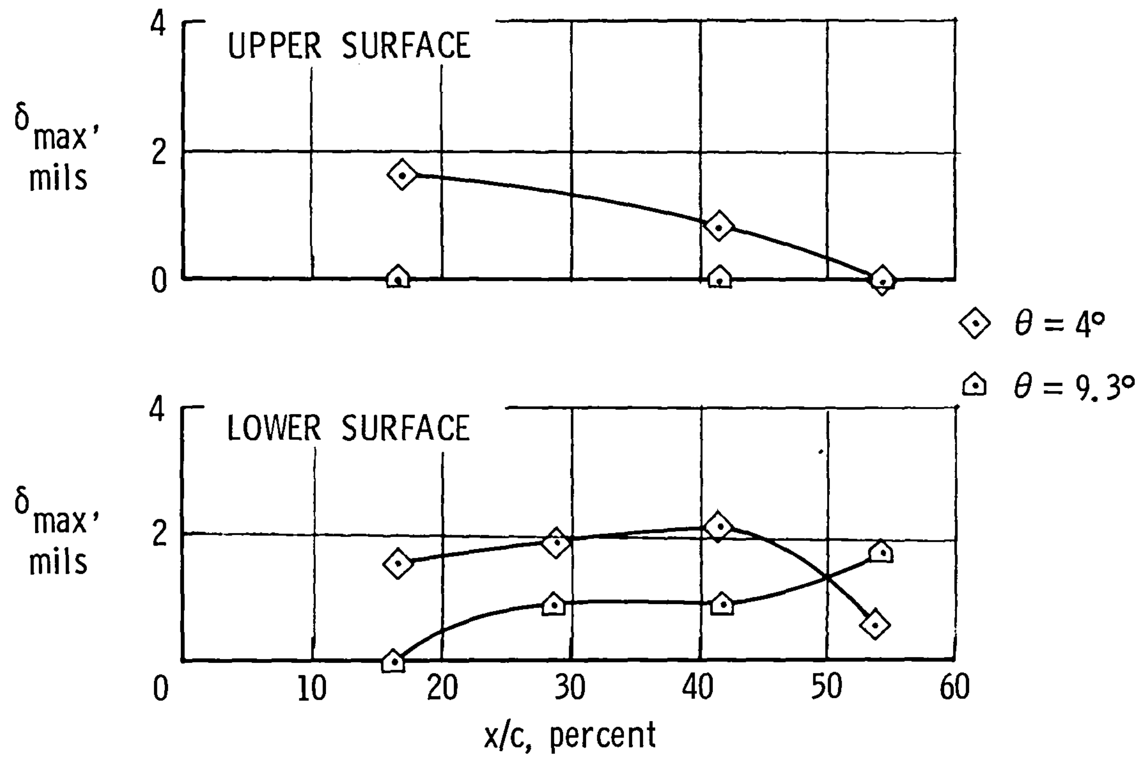

Figure 14.- Effect of pitch attitude on film thickness distribution. U = 112 ft/sec; Q = 3 gal/min.

1. Report No.	2. Government Accession No.	3. Recipient's Catalog No.
NASA TM-85796		

4. Title and Subtitle	5. Report Date
PRELIMINARY INDICATIONS OF WATER FILM DISTRIBUTION AND THICKNESS ON AN AIRFOIL IN A WATER SPRAY	July 1984
	6. Performing Organization Code 505-45-13-01
7. Author(s) Earl C. Hastings, Jr., and Leonard M. Weinstein	8. Performing Organization Report No. L-15767
	10. Work Unit No.
9. Performing Organization Name and Address NASA Langley Research Center Hampton, VA 23665	11. Contract or Grant No.
	13. Type of Report and Period Covered Technical Memorandum
12. Sponsoring Agency Name and Address National Aeronautics and Space Administration Washington, DC 20546	14. Sponsoring Agency Code

15. Supplementary Notes

16. Abstract

Preliminary results are presented from a test to evaluate a sensor for measuring water film thickness. The test was conducted at the Langley Research Center in a small flow apparatus with a 1-ft-chord model wing in a water spray. Photographic and visual observations were made of the upper wing surface and film thickness was measured on the upper and lower wing surfaces. Ahead of the wing, a bow wave of water droplets was observed. On the upper wing surface, a continuous water film formed, with the maximum thickness located at 16.7 percent of the chord length. Between 16.7 and 41.7 percent of the chord length, this continuous film broke down into many discrete runoff streams extending to the wing trailing edge. Measurements on the lower wing surface showed that, in general, the continuous film extended further aft than on the upper surface and that the maximum film thickness was located at 54.2 percent of the chord length. Increasing the flow velocity or increasing wing pitch attitude significantly decreased the thickness of the continuous film. The performance of the sensor appeared to be highly satisfactory, and where valid comparisons could be made, repeatable results were obtained.

17. Key Words (Suggested by Author(s))	18. Distribution Statement
Wing surface contamination Heavy rain effects Surface film measurements Surface film characteristics	Unclassified - Unlimited Subject Category 02

19. Security Classif. (of this report)	20. Security Classif. (of this page)	21. No. of Pages	22. Price
Unclassified	Unclassified	19	A02

National Aeronautics and
Space Administration

Washington, D.C.
20546

Official Business
Penalty for Private Use, $300

THIRD-CLASS BULK RATE

Postage and Fees Paid
National Aeronautics and
Space Administration
NASA-451

U.S.MAIL

NASA

POSTMASTER: If Undeliverable (Section 158
Postal Manual) Do Not Return